Kinetics and Catalysis, Vol. 42, No. 6, 2001, pp. 813–820. Translated from Kinetika i Kataliz, Vol. 42, No. 6, 2001, pp. 890–898.

The Relationship between the State of Active Species in a Ni/Al_2O_3 Catalyst and the Mechanism of Growth of Filamentous Carbon[1]

V. I. Zaikovskii, V. V. Chesnokov, and R. A. Buyanov

Boreskov Institute of Catalysis, Siberian Division, Russian Academy of Sciences, Novosibirsk, 630090 Russia

Received November 29, 2000

Abstract—The formation of active particles and their changes in the course of 1,3-butadiene decomposition on a Ni/Al_2O_3 catalyst at temperatures from 400 to 800°C were studied by high-resolution electron microscopy. It was found that carbon filaments of different types were formed at 400–800°C. The growth of thin filaments (20–30 nm in diameter) takes place at 400–600°C on a conical Ni particle located at the growing end of the filament, whereas di-symmetrical filaments 50–100 nm in diameter grow on biconical metal particles. As the carbonization temperature was increased to 700–800°C, graphite nanotubes 5–20 nm in diameter were formed. It was found that the mechanism of formation and the structure of filaments are related to the state of catalytically active species, which consist of a solid solution of carbon in the metal. It is suggested that the metastable surface nickel carbide Ni_3C_{1-x} is an intermediate compound in the catalytic formation of graphite filaments from 1,3-butadiene. Upon termination of the reaction, the metastable Ni_3C_{1-x} microphase is decomposed with the formation of hexagonal nickel microinclusions. The role of epitaxy in the nucleation and growth of a graphite phase on the metal is discussed. Models are presented for the growth of structurally different carbon filaments depending on the formation of active metal species at various temperatures. Considerable changes in the structure of carbon and the formation of nanotubes at 700–800°C are related to the appearance of a viscous-flow state of metal–carbon particles.

INTRODUCTION

Recently, studies of various types of thin carbon filaments obtained on catalysts that contain Ni, Fe, and Co metals and their alloys have been receiving increasing attention. Carbon filaments of the graphite structure are formed in the decomposition of hydrocarbons, in the disproportionation of CO, and in other reactions. It was found that the growth of filaments on metal particles occurs by a carbide cycle mechanism [1, 2]. According to this mechanism, a metastable carbide-like intermediate compound is produced on the decomposition of a hydrocarbon at the surface of an active particle. The degradation of this intermediate results in the formation of carbon, which further diffuses through the metal to the sites of crystallization into a graphite phase with the morphology of filaments. As a rule, a metal particle with a size of several tens of nanometers is arranged at one of the ends of a growing filament. Available data indicate that at carbonization temperatures of 400–600°C, active metal particles often exhibit clearly defined faces and different faces fulfill different functions in the main steps of the mechanism—the decomposition of a hydrocarbon and the formation of a graphite phase [2–7]. Data on the structural heterogeneity of active particles in catalysts and on the occurrence of carbide phases, along with metals, in these particles were published [6, 7]. However, information on the state of an active zone of the catalyst particle that includes carbide-like compounds, which are intermediates in the formation of a carbon phase in the course of hydrocarbon decomposition, and on the role of the microstructure of this zone is almost absent.

Carbon filaments obtained on catalysts widely vary in size, morphology, and structure [2–9]. Their length ranges up to a few tens of micrometers, and their diameters vary from tens to hundreds of nanometers. The hexagonal graphite (002) layers tilted to the direction of filament growth form the "fish-bone" filament structure [9]. Layers perpendicular to the direction of growth are detected in carbon filaments obtained by methane decomposition on nickel–copper alloys. In these cases, filaments with the "octopus" structure of branched graphite are formed [10, 11]. Recently, carbon fibers with layers parallel to the direction of growth (nanotubes) have attracted particular interest. The most disperse nanotubes are produced in a carbon plasma generated by an electric discharge or laser radiation [12–14]. However, a great number of concomitant carbon products from fullerenes to amorphous carbon or crystalline bulk graphite are formed in this case. The catalytic production of nanotubes, as well as other filaments, is preferable from the standpoint of controllable target-oriented preparation processes.

[1] Presented at the Memorial Yu.I. Ermakov Seminar on New Approaches to Purposeful Synthesis and Studies of Catalytic Systems (Novosibirsk, June 6–8, 2000).

0023-1584/01/4206-0813$25.00

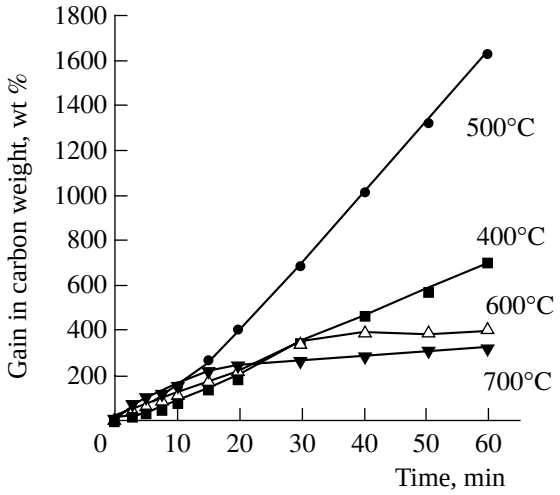

Fig. 1. Kinetic curves of carbon formation from 1,3-butadiene at various temperatures.

This work was devoted to the effect of the state of an active particle (structure, morphology, and phase composition) on the mechanism of growth of carbon filaments in hydrocarbon decomposition. These problems were solved in a study of the formation of carbon filaments from 1,3-butadiene on a highly dispersed Ni/Al_2O_3 catalyst by high-resolution electron microscopy (HREM).

EXPERIMENTAL

The mechanochemical activation of NiO and $Al(OH)_3$ powders was used for the preparation of Ni/Al_2O_3 catalyst samples. The reduction and carbonization of a catalyst composed of 90 wt % Ni/10 wt % Al_2O_3 was performed in a reactor with the Mac-Ben balance under gradientless conditions with respect to hydrocarbon concentration in the reaction mixture. The catalyst was reduced on heating in a hydrogen flow to 550°C for 20–30 min; thereafter, the sample was cooled or heated in argon to the required temperature of carbonization. The carbonization of the catalyst was performed in 1,3-butadiene diluted with argon and hydrogen in the molar ratio $C_4H_6 : H_2 : Ar = 2 : 40 : 75$ in a temperature range of 400–800°C. The dilution with argon and hydrogen was used for preventing the polymerization and condensation of butadiene and for activating the growth of filamentous carbon, respectively [2].

Rates of carbon formation (w) on a Ni/Al_2O_3 catalyst at various carbonization temperatures and times

Time, min	w, g C (g Cat)$^{-1}$ min^{-1}			
	400°C	500°C	600°C	700°C
0	0	0.05	0.18	0.25
10	0.10	0.20	0.11	0.12
30	0.12	0.30	0.07	0.02
60	0.12	0.30	0	0

The samples after carbonization were examined on a JEM-2010 high-resolution electron microscope with a line resolution of 0.14 nm and an accelerating voltage of 200 kV. A goniometer was used for obtaining images from required crystal orientations.

RESULTS AND DISCUSSION

Figure 1 demonstrates the kinetic curves of carbon formation from 1,3-butadiene at various temperatures. The table summarizes the rates of carbon buildup at different temperatures and carbonization times.

The catalyst was stable in operation at 400–500°C, whereas its activity decreased to almost zero after 0.5 h at higher temperatures (Fig. 1). In the initial period, the rate of carbon formation increased with reaction temperature. However, at 600°C, a rate higher than that at 500°C was observed for only a few minutes ($t < 10$ min). Thereafter, the rate of carbonization at 600°C dramatically decreased. As the temperature was further increased, the catalyst stability became lower. Carbon grew most intensely at a temperature of 500°C. In this case, the catalyst was relatively stable in operation for several tens of hours with the resulting yield of carbon of ≈10000 wt % relative to the initial catalyst weight.

The activation energies of the process were determined. At 380°C, the activation energy is 96 kJ/mol, which corresponds to the formation of nickel carbide [2]. At carbonization temperatures of 400–600°C, the activation energy of the process is 130–150 kJ/mol, which is consistent with the activation energy of carbon diffusion through nickel [15].

According to data from the electron microscope, the initial uncarbonized catalyst reduced in hydrogen at 550°C consists of almost uniform nickel metal particles isometric in shape with a particle size of 10–20 nm; these particles are separated by the interlayers of alumina particles. According to electron-microdiffraction data, nickel exhibits a face-centered cubic (fcc) structure. However, active states of the metal are formed during the growth of carbon filaments at temperatures from 400 to 800°C; this process is accompanied by considerable changes in the morphology, size, and structure of the metal particles.

Carbonization at 400–600°C results in the formation of two types of carbon filaments 20–30 and 50–100 nm in diameter, respectively. Figure 2 demonstrates the micrograph of carbon filaments of these types. Thin filaments are strongly curved, and an active nickel particle is located at the end. This nickel particle exhibits the morphology of a truncated drop or cone with the basal plane faced toward the direction of filament growth (Figs. 3a, 3b). As a rule, the diameter of the metal particle is equal to the diameter of the carbon filament, and the length is 30–50 nm. The growth of a graphite phase

as filaments occurs at the cone portion of the particle. As follows from the HREM image in Fig. 3b, graphite in the filaments exhibits a defect structure, in which the (002) layers form cones arranged at 30°–45° angles to the direction of filament growth (fish-bone structure). At a carbonization temperature of 400°C, thin filaments do not contain internal cavities, whereas an increase in the temperature to 500–600°C results in the appearance of hollow channels within filaments. These channels contain rare carbon crosspieces of one or two graphite monolayers. The channel diameter varied from 1/8 to 1/4 of the external diameter of the filament.

Thicker carbon filaments 50–70 nm in diameter, which are formed at 400–600°C, consist of two oppositely directed branches. Metal particles are biconical in shape, and they are located at the middle of the filaments symmetrically with respect to the branches (Fig. 4a). The diameter of the metal particle corresponds to the diameter of the carbon filament, and the longitudinal dimension is 100–300 nm. The structure of carbon filaments of this type is determined by the biconical shape of the surface of metal particles, and it is formed by graphite layers tilted to the direction of growth (Figs. 4b, 4c). According to data from the electron microscope, the mass fraction of thin filaments in samples prepared at 400–600°C is approximately equal to the fraction of thick filaments, and it remained unchanged with carbonization time.

Only one type of carbon filaments was formed at higher temperatures of 700–800°C. These are extremely thin multilayer graphite nanotubes with external diameters of 5–20 nm and hollow internal channels 2–5 nm in diameter (Fig. 5). The graphite layers are almost parallel to the axis of the tube and they are cylindrical in shape. Hollow channels measure about 1/4 of the external diameter of a nanotube. Metal particles located at the ends of the filaments are round shaped. A portion of the metal is carried out to the hollow channels of the tubes as cylindrical inclusions up to 10 nm long.

Figure 6 schematically depicts the types of metal inclusion particles, their location in carbon filaments, and the structures of filaments obtained at various temperatures.

Note that low-activity nickel particles are formed along with active particles in the decomposition of 1,3-butadiene. In these cases, composite reaction products, bulk metal particles (more than 100 nm) coated with a thick layer of carbon, are detected in the samples (Fig. 5a). The fraction of these particles increases as the reaction temperature is increased from 600 to 800°C.

The HREM images of catalysts carbonized at 400–500°C (Figs. 3b, 4b) are indicative of the structural heterogeneity of metal particles located in carbon filaments. The greater part of the volume of particles located at the ends of thin carbon filaments consists of nickel with the fcc structure. The conical surface of cubic nickel is in contact with carbon. The frontal flat surface, which is an active zone of the particle, is free of carbon; the hydrocarbon decomposes at this surface. The structure of the particle is changed near the frontal surface; here, a flat inclusion of hexagonal nickel with a thickness of about 3 nm was detected (Fig. 3b). The determination of crystalline phases in such small-size single inclusions by measuring the lattice spacings is usually ambiguous. Therefore, we performed the comparative identification of hexagonal and cubic nickel modifications by a comparison of experimental HREM images with theoretically calculated patterns [16]. Figure 3c demonstrates the agreement between simulated and experimental images. The direction [001] of hexagonal nickel coincides with the diagonal direction [111] of cubic nickel, which is oriented along the direction of growth of the carbon filament. In these directions, the atomic lattices of both of the nickel modifications exhibit hexagonal symmetry and closely correspond to each other (the interatomic distances are d_{110} = 0.249 nm and $2 \times d_{110}$ = 0.265 nm for cubic and hexagonal nickel, respectively). In the region of the transition from the hexagonal metal phase to the cubic phase, we also detected polytwins of cubic nickel with the interfaces parallel to the frontal plane of the metal particle.

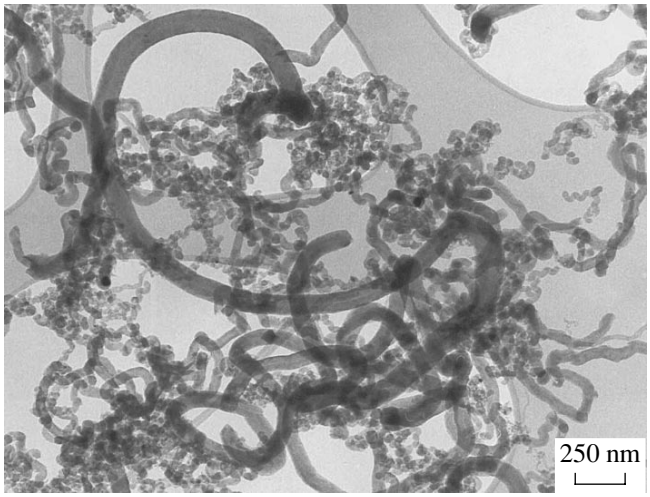

Fig. 2. Carbon filaments in a catalyst carbonized at 400°C.

The active zones of biconical catalyst particles, which were detected at 500–600°C, exhibit another structure. Symmetrical carbon fibers 50–100 nm in diameter grow at these particles. In this case, the uncovered portions of the surface in the middle of the particle (at the site of the passage of its plane of mirror symmetry) are active in hydrocarbon decomposition. According to data from the electron microscope, particles of a hexagonal nickel microphase were detected at these sites; these particles circularly surround a biconical particle (Fig. 4b). The HREM images clearly demonstrate the crystal lattice of microphase particles having the polycrystalline structure. The lattice spacings measured from the HREM micrographs (d_n: 0.23, 0.22, and

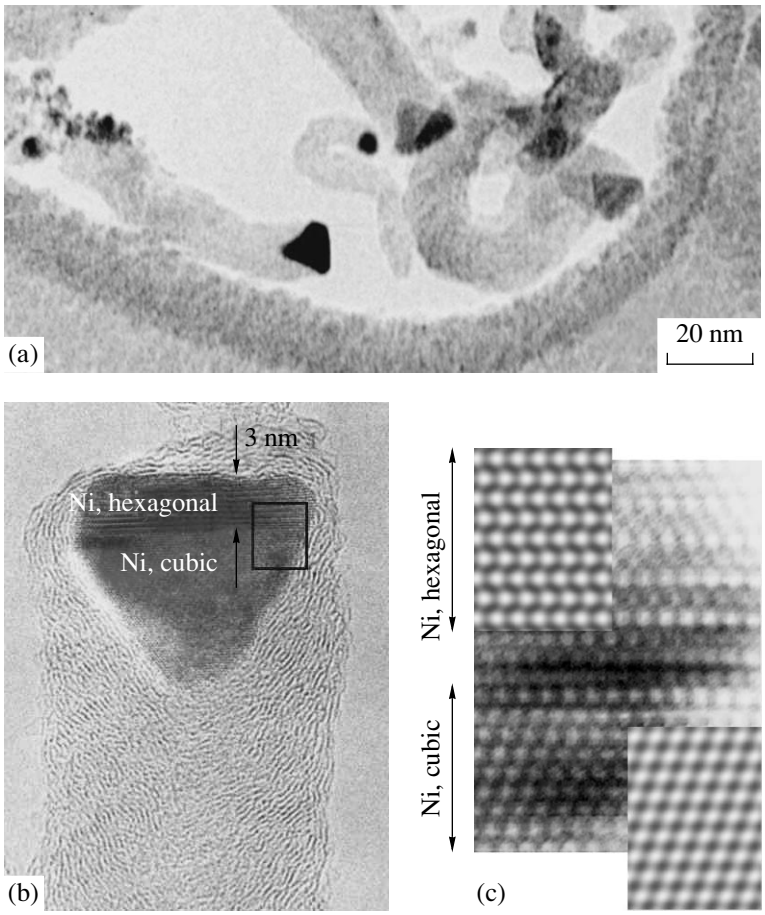

Fig. 3. Ni/Al_2O_3 catalyst carbonized at 400°C. (a) Thin carbon filaments 20–30 nm in diameter containing a teardrop-shaped nickel particle at the end. (b) The structure of a carbon filament and a metal inclusion particle. (c) The magnified framed fragment of the HREM image in Fig. 3b. Insets: simulated images of the atomic structures of hexagonal nickel [100] (top) and cubic nickel [110] (bottom), which correspond to the images obtained with an electron microscope.

0.20 nm) correspond to the hexagonal modification of nickel.

It is of interest to consider contact zones between conical metal surfaces and carbon for elucidating the mechanism of graphite crystallization at the surface of a metal particle. A study of metal–graphite interfaces demonstrated that the metal surface here exhibits both smooth conical portions denoted by A in Fig. 4c and irregularities or steps by B, which are usually no greater than 1 nm in height. As a rule, the smooth portions are formed by vicinal planes (i.e., different in orientation from the main singular faces); however, they often represent the (111) crystal faces of fcc nickel.

Graphite contacts the smooth conical surface of a metal particle through basal planes so that the graphite (002) layers are almost parallel to the metal surface. This arrangement of graphite layers is responsible for the formation of a filament structure as the embedded cones of graphite monolayers (fish-bone structure). It is well known that the fcc metal (111) planes and the graphite (002) planes exhibit the same hexagonal symmetry, and interatomic distances in the hexagonal lattices of nickel (d_{110} = 0.249 nm) and graphite phases ($2 \times d_{110}$ = 0.246 nm) are almost equal. Evidently, the similarity of structural parameters is favorable for the appearance of epitaxial contact regions of graphite on nickel.

Figure 4b demonstrates the HREM image of the boundary of graphite with a biconical metal particle. It follows from the image that another type of graphite epitaxy on nickel takes place at the steps of the conical surface of the particle. In this case, the ends of the (002) planes rather than the planes are in contact with the metal at the steps of the conical surface of the particle. In this situation, a prerequisite to epitaxy is the close correspondence of the interlayer parameter d_{002} = 0.34 nm of graphite to the doubled parameter d_{100} = 0.175 nm of the metal (0.175 nm × 2 = 0.35 nm); that is, for two metal (100) layers there is one graphite (002) layer.

Thus, epitaxial conditions for the growth of graphite occur at both the flat (111) faces of fcc nickel and the steps of the (100) planes on the conical surface of the metal. It is well known [17] that the epitaxy of related

phases decreases the interfacial energy and facilitates the epitaxial growth of the growing phase.

According to HREM data, after carbonization at 700–800°C, cubic nickel particles were also located at the ends of nanotube filaments and within their hollow channels. This is evident from the lattice spacings that correspond to this phase (d_n: 0.205 and 0.175 nm). Hexagonal inclusions were not detected in these particles. The frontal surface of a metal particle is open, and the opposite surface is in contact with the edges of the graphite (002) layers of nanotubes (Fig. 5c).

Thus, we found that carbon filaments, which are significantly different in size, morphology, and structure, are formed by the decomposition of 1,3-butadiene on dispersed Ni/Al_2O_3 catalysts within a temperature range of 400–800°C. These differences in properties resulted from changes in the states of catalyst metal particles incorporated in the filaments. We consider the appearance of these active states from the standpoint of the mechanism of formation of carbon filaments. Previously [1, 2], a cyclic carbide mechanism of the growth of carbon filaments from hydrocarbons on iron-subgroup metal particles was schematically presented as follows:

$$\text{Ni} \xrightarrow{C_4H_6} |\text{Ni–C}| + H_2 \longrightarrow \text{Ni} + \text{C} + \text{graphite}.$$

According to this mechanism, an unstable carbide-like state |Ni–C|, which appears in hydrocarbon decomposition, decomposes to the metal and carbon, and carbon atoms entering the bulk metal form a supersaturated of carbon in the metal. When a critical supersaturation was attained, the nuclei of the graphite phase were formed at specific sites of the surface of metal particles and graphite filaments began to grow. The mass transfer of carbon occurred by diffusion through the bulk particle under the effect of a carbon concentration gradient. This diffusion was directed from the particle surface site active in hydrocarbon decomposition to the sites of the growth of a graphite phase. The agreement between the activation energy of reactions and the activation energy of carbon diffusion through the metal ($E_a \approx 130$–150 kJ/mol) demonstrated that the diffusion of carbon is the rate-limiting step of the formation of filaments from 1,3-butadiene on a Ni/Al_2O_3 catalyst at 400–500°C. Below 400°C, a phase of the nickel carbide Ni_3C is formed ($E_a = 96$ kJ/mol).

It follows from electron microscopic data that hexagonal nickel microphase inclusions, which are structurally different from the bulk of the particles, are located at the active sites of the surface of catalyst particles removed from the reactor. It is necessary to explain the reason why the hexagonal modification of nickel was detected, although it is well known that the cubic metal is more stable at temperatures higher than 380°C [19, 20].

It is well known that the ideal crystalline phase of Ni_3C is inactive in the decomposition of hydrocarbons

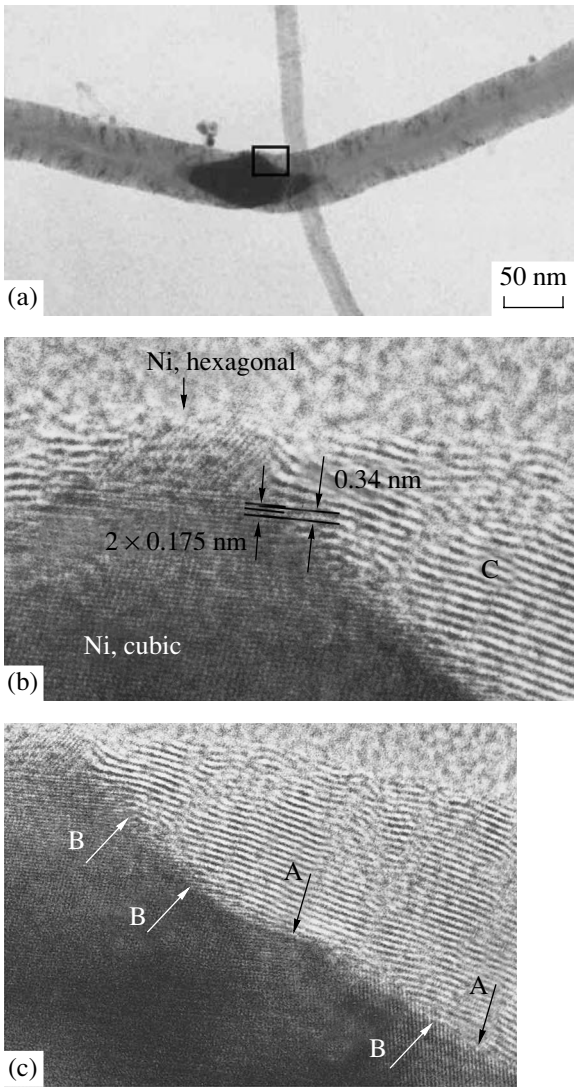

Fig. 4. Ni/Al_2O_3 catalyst carbonized at 500°C. (a) Thick carbon filaments consisting of two branches. The metal particle exhibits a symmetrical biconical shape, and it is arranged symmetrically with respect to the two branches of the filament. (b) The HREM micrograph of the active zone of a metal particle and epitaxial contact between the metal and a graphite phases (magnified framed fragment of Fig. 4a). (c) The contact between graphite and the uneven surface of a conical metal particle: (A) planes (002) are parallel to the metal surface; (B) the edges of graphite layers are in contact with the metal.

[1]. The hexagonal carbide Ni_3C has a sublattice of metal atoms, which is almost identical to the lattice of hexagonal nickel metal [19, 21], and carbon atoms in the carbide occupy a third of the octahedral voids in the metal sublattice. Ni_3C is unstable, and it decomposes into the hexagonal metal and carbon even at 400°C [20]. Thus, the formation of a metastable carbidelike compound on the open surface of a metal particle should be expected in the reaction with a hydrocarbon at temperatures higher than 400°C. This carbide-like

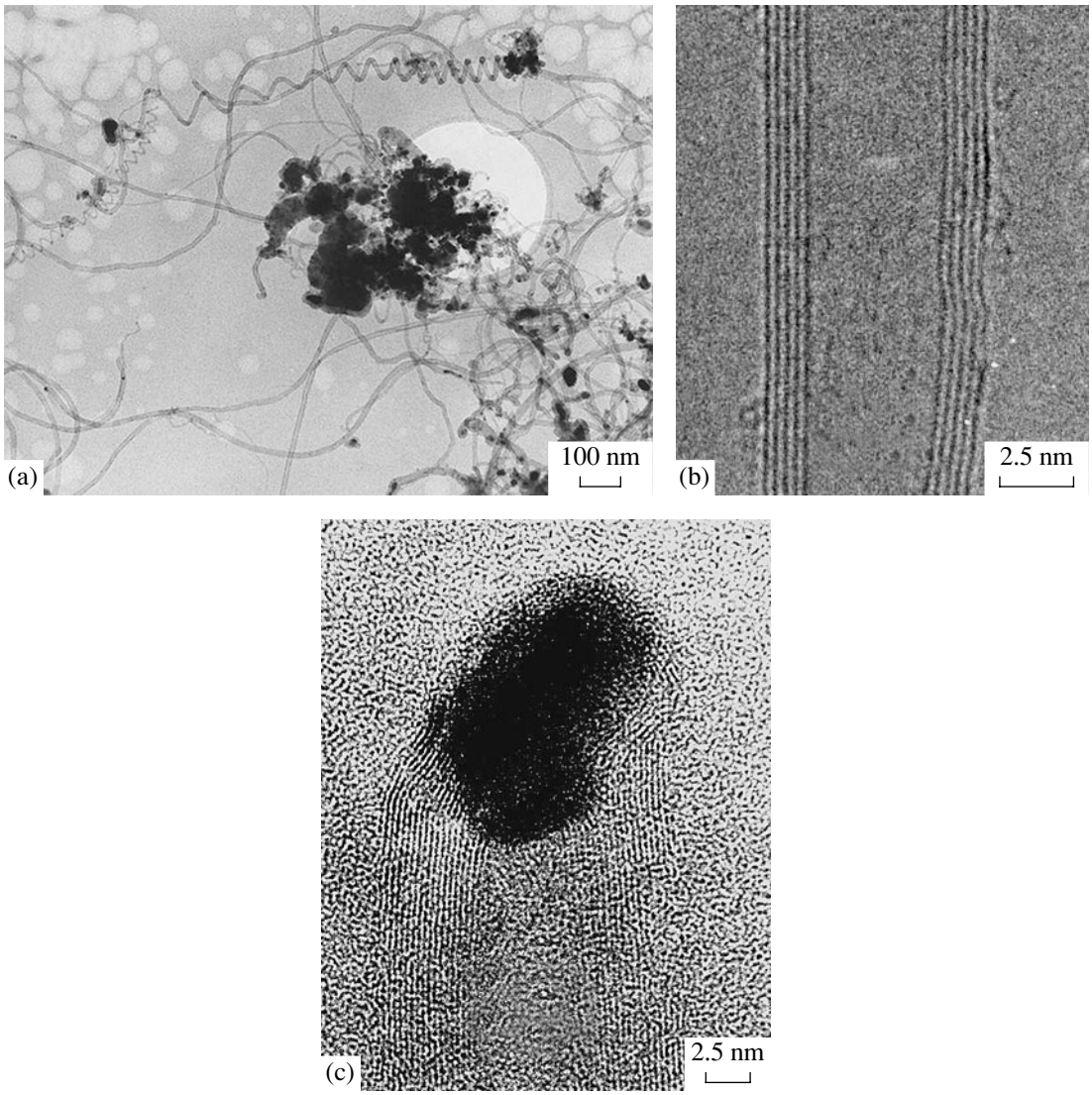

Fig. 5. Ni/Al_2O_3 catalyst carbonized at 750°C. (a) Nanotubes and coarsely dispersed graphite. (b) The structure of a nanotube with the graphite layers (002) arranged in parallel with the axis of the tube. (c) Location of a metal inclusion at the end of the nanotube.

compound with a metal-to-carbon ratio close to 3 : 1 is the nonstoichiometric defect nickel carbide Ni_3C_{1-x}. The carbide-like microphase occupies a very small volume, and its dimensions depend on a balance between the rates of its formation in the reaction of the hydrocarbon with the metal and of decomposition into the metal and carbon. Carbon that appears in the decomposition of the unstable carbide forms a supersaturated solution of carbon in the metal.

The carbide-like microphase of Ni_3C_{1-x} can occur only under nonequilibrium conditions of a chemical reaction, and the termination of the reaction results in the degradation of this microphase. After the reaction, nickel metal in a hexagonal modification remained at the site of microphase location near the frontal surface of the particle, whereas the cubic metal resided in the bulk of the particle. Carbon was present in the metal in a dissolved form.

The hexagonal and cubic packings of the metal consist of identical closely packed flat hexagonal atomic layers, and they only differ in the sequence of alternating layers: ABCABC… or ABABAB… in the cubic or hexagonal packing, respectively. As we found in [4, 5], the structural similarity of flat atomic layers is favorable for the epitaxy of phases, as well as for polytypic transitions and twinning in nickel particles. Such structures were observed near the frontal surface of teardrop-shaped metal particles of size 20–30 nm in catalyst samples carbonized at 400–600°C. The structure of the particle becomes more regular as the distance from the frontal surface increases, and the tail end contains no visible defects.

The data from the electron microscope demonstrated that the interaction with the hydrocarbon at 400–800°C results in the appearance of active metal states and in considerable changes in their morphological and structural properties. Self-organization phenomena occur in the labile metal–carbon system; these phenomena manifest themselves in the formation of metal particles that are optimal for the growth of carbon filaments of different sizes and structures. During the growth of a filament, the formed graphite planes slide over the metal surface, and the transfer of nickel atoms in the direction of the diffusion flow of carbon atoms is intensified [2]. As a result, the particle is stretched and a conical surface is formed whose vertex is facing away from the direction of filament growth. The metal particles shaped like a truncated cone are about 20 nm in size, whereas the size of biconical particles is 50–100 nm. The metal particle size completely determines the diameters of carbon filaments that originate from this particle. In the case of a small particle, atomic carbon diffuses from the face where 1,3-butadiene decomposes to the conical surface where the graphite phase is formed. In the second case, thicker filaments can be formed on biconical particles because a great number of hydrocarbon degradation centers occur at the entire periphery of the bases of adjacent cones. Carbon simultaneously grows as two symmetrical branches from the opposite sides of the catalyst particle. This shortens the diffusion distances of carbon atoms from the sites of hydrocarbon decomposition to the sites of crystallization into a graphite phase, as noted in [4, 5], for the growth of filaments on Ni–Cu/Al_2O_3 and Ni–Pd/Al_2O_3 catalysts.

We explain the lability of particles by the appearance of viscous-flow properties, which are similar to the properties of liquids, in solid particles. Evidently, the metal particle is heated because the heat of condensation is released when carbon atoms pass from a solution in the metal to a graphite phase. However, a simple calculation demonstrates that this heating is insignificant and the temperature increases by only a few degrees Celsius [22]. The formation of a labile state is facilitated by the enhanced ability of crystal lattice atoms to migrate (self-diffusion). This ability is associated with the fact that, under nonequilibrium reaction conditions and at a high carbon concentration in the metal, fast carbon transport through the crystal leads to strong nonthermal atomic oscillations in the metal lattice [3, 15].

In connection to this, the appearance of coarsely dispersed metal states along with active species at carbonization temperatures of 600–800°C can be explained by the fact that the lability properties of the system of particles are more pronounced at high temperatures. In this system, the agglomeration of particles and the transformation of a portion of the metal into a coarsely dispersed state even occur in the induction period of the reaction. In this case, bulk metal particles (greater than 100 nm) covered with a thick carbon layer are formed. These states are inactive because the appearance of high carbon concentration gradients in bulky metal particles and the transport of carbon to the graphite-phase nucleation sites are impossible.

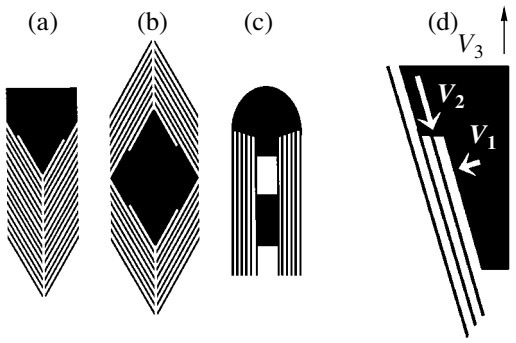

Fig. 6. Types of nickel metal particles in carbon filaments and the orientation of graphite layers at the sites of contact with the metal surface: (a) metal particle at the end of a filament with the fish-bone structure; (b) metal particle at the middle of symmetrical filament branches with the fish-bone structure; (c) metal particles at the end of a nanotube and within its hollow channel; and (d) graphite growth at the stepped conical metal surface tilted to the direction of filament growth; V_3 is the velocity of filament growth, V_1 is the component of the velocity of graphite formation perpendicular to the conical surface, and V_2 is the tangential component.

In a study of the interaction of graphite with the surface of nickel particles, we found that, in addition to the location of the closely packed graphite (002) layers in parallel with the metal surface, graphite grows at the surface steps, contacting with them at the edges of the (002) layers (Fig. 6c). This allows us to explain why carbon filaments grow on the metal surfaces tilted to the direction of growth (velocity vector V_3, Fig. 6d). Indeed, the notion of carbon growth due only to the addition of a number of graphite layers in stacks can explain the growth of carbon only perpendicularly to the metal surface (V_1). The growth of graphite (002) layers on the side of their edges at the steps of the metal surface explains the appearance of the tangential component V_2 of the velocity of graphite-phase growth and the agglomeration of layers into a graphite filament, which remains behind the metal particle in the growth of filaments with the fish-bone structure (400–600°C).

In the growth of nanotubes with parallel carbon layers (600–800°C), the epitaxial growth of graphite contacting with the metal surface at the edges of the (002) layers is predominant (Fig. 6c). In this case, after the formation of graphite layers, they slide over the cylindrical surface of the metal particle and separate from the metal particle with the formation of a carbon nanotube. We detected no traces of a carbide-like compound microphase in the samples prepared at 700–800°C. Of course, the decomposition of the metastable phase of a carbide-like compound becomes predominant in a balance between the rates of formation and decomposition at high reaction temperatures. It is believed that reac-

tion intermediates like Me_xC_y occur on the active metal surface at these temperatures only in molecular form, they cannot be detected using an electron microscope.

It is not improbable that such dramatic changes in the properties of carbon filaments and metal particles at reaction temperatures of 700–800°C are associated with the fact that, at these temperatures, the fluidity of active metal–carbon particles (size of 5–20 nm) is considerably enhanced. The fluid properties of the particles approach the properties of liquids at temperatures much lower than the melting temperature of the eutectics of carbon with the metal [22, 23]. Direct evidence for a change in the state of aggregation of the particles can only be obtained with the use of *in situ* high-resolution electron microscopy.

ACKNOWLEDGMENTS

This work was supported by the Russian Foundation for Basic Research (project no. 99-03-32420) and the Program "Leading Scientific Schools of Russia" (project no. 00-15-7440).

REFERENCES

1. Buyanov, R.A., *Zakoksovanie katalizatorov* (Catalyst Coking), Novosibirsk: Nauka, 1983.
2. Chesnokov, V.V. and Buyanov, R.A., *Usp. Khim.*, 2000, vol. 69, no. 7, p. 675.
3. Baker, R.T.K. and Harris, P.S., *Chemistry and Physics of Carbon*, New York: Marcel Dekker, 1978, vol. 14, p. 83.
4. Zaikovskii, V.I., Chesnokov, V.V., and Buyanov, R.A., *Kinet. Katal.*, 1999, vol. 40, no. 4, p. 612.
5. Zaikovskii, V.I., Chesnokov, V.V., Buyanov, R.A., and Plyasova, L.M., *Kinet. Katal.*, 2000, vol. 41, no. 4, p. 538.
6. Audier, M., Oberlin, A., and Coulon, M., *J. Cryst. Growth*, 1981, vol. 55, p. 549.
7. Kim, M.S., Rodriges, N.M., and Baker, R.T.K., *J. Catal.*, 1991, vol. 131, p. 60.
8. Baker, R.T.K. and Rodrigues, N.M., *Proc. Material Research Society Symp.*, Bernier P. *et al*., Eds., Pittsburgh, 1995, vol. 359.
9. Fenelonov, V.B., Derevyankin, A.Yu., Zaikovskii, V.I., *et al.*, *Carbon*, 1997, vol. 35, no. 8, p. 1129.
10. Bernardo, C.A., Alstrup, I., and Rostrup-Nielsen, J.R., *J. Catal.*, 1985, vol. 96, p. 517.
11. Chesnokov, V.V., Zaikovskii, V.I., Buyanov, R.A., *et al.*, *Kinet. Katal.*, 1994, vol. 35, no. 1, p. 146.
12. Iijima, S., *Nature*, 1991, no. 354, p. 56.
13. Journet, C. and Bernier, P., *Appl. Phys. A*, 1998, vol. 67, p. 1.
14. Thess, A., Lee, R., Smalley, R.E., *et al.*, *Science*, 1996, no. 273, p. 483.
15. Chesnokov, V.V., Buyanov, R.A., and Zaikovskii, V.I., *Khim. Interes. Ust. Razv.*, 1997, vol. 5, no. 6, p. 619.
16. Gruzin, P.L., Polikarpova, Yu.A., and Fedorov, T.B., *Fiz. Met. Metalloved.*, 1975, vol. 4, no. 1, p. 94.
17. Cowlrey, J.M., *Diffraction Physics*, Amsterdam: North Holland, 1972.
18. Palatnik, L.S. and Papirov, I.I., *Orientirovannaya kristallizatsiya* (Oriented Crystallography), Moscow: Metallurgiya, 1964.
19. Nagakura, S., *J. Phys. Soc.*, 1957, vol. 12, no. 5, p. 482.
20. Bahr, H.A. and Bahr, Th., *Ber. Deut. Chem. Gesel*, 1928, vol. 61, p. 2177.
21. Carturan, S., *Mater. Lett.*, 1988, vol. 7, p. 47.
22. Krivoruchko, O.P., Zaikovskii, V.I., and Zamaraev, K.I., *Dokl. Akad. Nauk*, 1993, vol. 329, no. 6, p. 744.
23. Parmon, V.N., *Catal. Lett.*, 1996, vol. 42, nos. 3–4, p. 195.